Global Ecology and Biogeography

WILEY

Global Ecology and Biogeography | A Journal of Macroecology

RESEARCH ARTICLE

The Impact of Disturbance on Tree Size Distributions in the United States

Adam J. Eichenwald[1,2] | John M. Grady[1,2] | Jonathan A. Knott[3] | Quentin D. Read[4] | J. Marcos Rodriguez[1,2] | Sydne Record[1,2]

[1]Department of Wildlife, Fisheries, and Conservation Biology, University of Maine, Orono, Maine, USA | [2]Maine Agricultural and Forest Experiment Station, Orono, Maine, USA | [3]USDA Forest Service, Northern Research Station, Forest Inventory and Analysis Program, Saint Paul, Minnesota, USA | [4]USDA Agricultural Research Service, Raleigh, North Carolina, USA

Correspondence: Adam J. Eichenwald (adam.eichenwald@maine.edu)

Received: 14 November 2024 | **Revised:** 16 June 2025 | **Accepted:** 22 July 2025

Handling Editor: Ines S. Martins

Funding: This work was supported by Northeastern States Research Cooperative. NASA Biodiversity and Ecological Conservation program, 80NSSC23K0421. U.S. Department of Agriculture National Institute of Food and Agriculture, MEO-022425.

Keywords: ecosystem dynamics | fire | forest inventory and analysis (FIA) | global forest changes | scaling predictions

ABSTRACT

Aim: Tree size distributions are an emergent feature of forest dynamics across space and time. Theory suggests that undisturbed forests exhibit a size-abundance distribution captured by a power-law relationship with a near-2 slope. We aimed to quantify how disturbances systematically and predictably cause deviations from this expected pattern.

Location: Contiguous United States.

Time Period: 2001–2023.

Major Taxa Studied: Diverse tree communities.

Methods: We analysed size-abundance distributions in over 160,000 FIA plots for both disturbed and undisturbed forests, examining changes in slope associated with disturbances, stand age, and maximum tree height. We used a Structural Equation Model (SEM) to evaluate whether disturbance effects on size-abundance slopes were indirectly mediated by changes in stand age or maximum height.

Results: We found that the predominant disturbances across the dataset (e.g., ground fires, animal damage) result in predictable flattening of size-abundance slopes, reflecting the selective removal of smaller trees. In contrast, many disturbances (e.g., wind, disease) did not shift the slopes predictably, indicating that they did not selectively impact any specific size class. Maximum tree height and stand age were also reliable predictors of size-abundance distributions, but a structural equation model demonstrated that the impact of disturbance on size-abundance slopes was not mediated through its indirect effects on stand age or maximum tree height, suggesting a direct pathway of influence.

Main Conclusions: Disturbances result in predictable changes to forest size-abundance slopes. As climate change and increased disturbance frequencies produce younger and shorter forests, future size-abundance slopes are expected to be steeper than those in undisturbed forests. Our findings suggest a temporary flattening in the size-abundance relationship immediately after the predominant disturbances across the dataset (ground fires, animal damage). These findings underscore the importance of understanding disturbance impacts on forest size structure to improve predictions of forests across broad spatial and temporal scales.

1 | Introduction

Tree size structure influences a range of patterns and processes in forest ecosystems, including carbon sequestration, habitat availability, and nutrient cycling (Piponiot et al. 2022). Consequently, models that predict tree size distributions are crucial tools for forecasting forest dynamics under increasing disturbances (Piponiot et al. 2022). Trees, like most organisms, become increasingly rare at larger sizes. Size distributions in forests are shaped by demographic processes like growth, mortality and recruitment, and are key predictive features in mechanistic models of forest structure (Farrior et al. 2016; Grady et al. 2024). Surprisingly, these size distributions exhibit regularity across diverse habitats, suggesting the presence of consistent rules governing tree sizes (Enquist et al. 2009; Farrior et al. 2016; Zhou et al. 2021; Grady et al. 2024).

Tree size distributions in forests typically follow a power law, often with a slope near-2 in a regression of tree frequency by stem diameter (Enquist et al. 2009; Zhou et al. 2021). The specific mechanism at work is still debated, but empirical tests indicate that, on average, the predicted scaling values do appear across sites (Belgrano et al. 2002; West et al. 2009; Zhang et al. 2015; Perkins et al. 2019; Zhou et al. 2021). West et al. (2009) proposed that-2 scaling represents a 'zeroth-orde' expectation for undisturbed forests at demographic equilibrium, where tree competition for space and mortality balances growth. However, disturbances may lead to deviation from this-2 slope expectation until the forest recovers (Figure 1). For example, fires may remove small trees from the forest, leading to shallower slopes before establishment of new saplings. Alternatively, windthrow events that remove large overstory trees and open up light in the understory may lead to a profusion of saplings and subsequently steeper slopes. Frequent disturbance has been argued to lead to systemic deviations from predicted-2 scaling for slopes (Coomes et al. 2003; Muller-Landau et al. 2006), although models have shown that small gap generation with associated light penetration may be essential to generating power law scaling of size distributions (Farrior et al. 2016).

Enquist et al. (2009) observed that stand-clearing disturbances may temporarily lead to a steeper size-abundance slope, with the virtual disappearance of large trees and an abundance of small trees released from competition for light. This pattern seems to hold across a large scale, as Duncanson et al. (2015) found that forests with shorter tree heights across the United States exhibited a substantially more negative deviation from the expected −2 slope, even after controlling for various environmental factors. Given the allometric relationship between tree height and size (taller trees generally have larger diameters), this suggests that forests dominated by smaller/shorter trees after a stand clearing disturbance in general tend to have size distributions that deviate more strongly from the theoretical equilibrium. Therefore, disturbances that alter the age structure and maximum height of a forest should predictably influence its size-abundance slope indirectly via these variables. While disturbances range in scale and frequency, from frequent small gaps to rarer stand-clearing events (Kellner and Asner 2009), the prevalence of high-intensity disturbances has increased due to shifts in forest management, land use change and climate change (Seidl et al. 2017). Given that disturbance is a consistent and increasingly important feature of forests globally, understanding its role in shaping forest size distributions is critical for elucidating the foundations of forest assembly, structure and dynamics (McDowell et al. 2020).

Here we examine the role of disturbances on the size-abundance scaling relationship of forests across the conterminous United States, controlling for the effect of forest treatments, using data gathered from the Forest Inventory and Analysis Program (FIA).

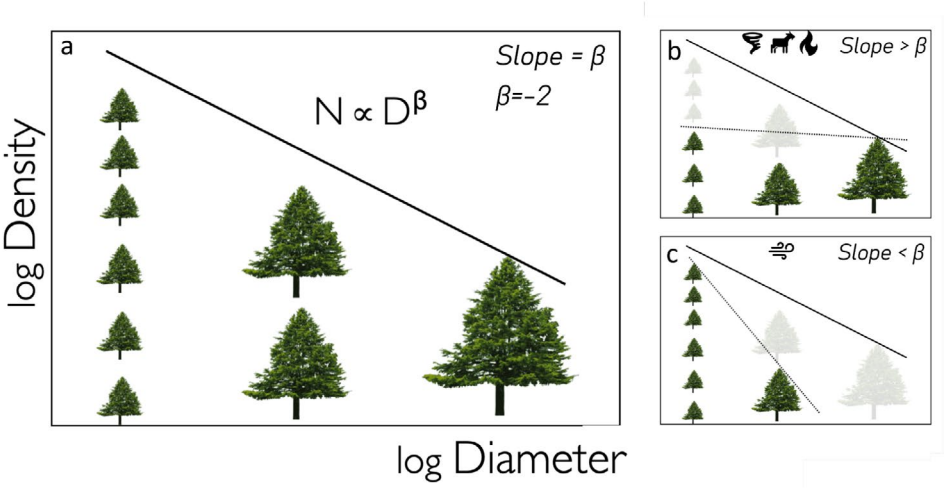

FIGURE 1 | Hypothetical impact of different disturbance types on the size-abundance relationship in forests. (a) Slopes of this relationship (with both axes log scaled) are considered to converge on −2 when the forest is in demographic equilibrium and is at a mature stand age (Enquist et al. 2009). (b) For disturbances that do not kill all trees but are more likely to destroy smaller trees, such as ground/surface fires or animal grazing, we expect the slope to flatten due to relative stability in the larger size classes. (c) For disturbances that do not kill all trees but are more likely to destroy taller trees, such as wind from microbursts, we expect the slope to steepen due to the relative stability in the smaller size classes. Finally, we expect high wind from storms and tornadoes to flatten slopes by destroying trees indiscriminately. In a, b and c solid lines represent −2 scaling expected for no disturbance, whereas in b and c dotted lines indicate size-abundance relationship with disturbance. While only one species is depicted in the conceptual diagram, actual size-abundance relationships in empirical data include all species present in a plot.

The FIA Program conducts the Nationwide Forest Inventory that systematically collects data on forest conditions, species composition, and changes over time across the United States, allowing for in-depth investigations of forests across broad temporal and spatial swaths. We explore the relationship between a variety of disturbance-related and environmental predictors and the size-abundance slopes of forest plots. We use structural equation models (SEMs) to disentangle the roles of disturbance and intrinsic forest characteristics (i.e., height and stand age) on the diameter size distributions of forests across the United States. We posit that disturbance will indirectly influence size-abundance slopes via stand age and maximum height. Finally, we hypothesise that disturbances primarily affecting smaller trees will result in shallower size-abundance slopes compared to undisturbed plots, whereas disturbances that reduce the abundance of trees of all sizes equally are unlikely to cause significant differences in slope (Figure 1).

2 | Materials and Methods

2.1 | FIA Overview

The FIA Program collects, publishes, and analyses data describing the extent, condition, volume, growth, and use of trees from all land ownerships in the nation (Smith 2002; Tinkham et al. 2018; Stanke et al. 2020). The FIA Program transitioned to the current 'annual' inventory in 1999, when FIA established a semi-systematic sample of ~350,000 plots across the contiguous U.S., AK, HI, and the U.S. Territories and Affiliated Islands. About 140,000 of these plots occur on forested land. Generally, 1/10 of plots are measured each year in the western U.S. and 1/7 or 1/5 of plots are measured each year in the eastern U.S., leading to a 10-year or 5–7-year remeasurement period in the west and east, respectively. In total, the FIA database includes ~16.8 million tree records from ~483,000 measurements of forested plots. Additionally, forest conditions (areas of the plot that are homogeneous with respect to parameters such as forest type and disturbance category, among others) are delineated by field crews, with ~726,000 condition records in the FIA database. FIA data have been widely utilised in macroscale forest ecology research (e.g., Fei et al. 2018; Tinkham et al. 2018; Knott et al. 2020) and a variety of national and international reports on the status and trends of forests across the U.S. (Oswalt et al. 2019; e.g., Domke et al. 2023). The FIA Program uses a nationally consistent plot design with four 7.31-m radius subplots (168 m^2), recording trees with diameter at breast height (DBH) $\geq$ 12.7 cm. Nested within each subplot are 2.07-m radius microplots (13.5 m^2), measuring trees with DBH < 12.7 cm (hereafter 'saplings'). Optional 17.9-m radius macroplots (1013 m^2) centred on the subplots are reserved for large trees (DBH generally > 50.8 cm) and are only used in the Pacific Northwest region.

2.2 | Size-Abundance Slopes

Abundance mapped by a power law typically extends from small saplings to canopy giants, but data on the smallest trees are not always available. In our case, microplots cover smaller areas, which means that abundance measurements of saplings are not directly comparable to trees measured in subplots. To account for this, we standardised abundance to a per-unit-area basis using the FIA-assigned trees per acre (TPA) expansion factor, which scales individual tree counts to an estimated number of trees per acre based on the ratio of sampling area to one acre of land (Bechtold and Patterson 2005). This factor, which FIA assigns individually to each tree, adjusts the individual tree counts from each plot to estimate the number of trees per acre, accounting for the specific size of the sampling areas used for each size class. By doing so, we ensure that the abundance of saplings, measured in smaller microplots, is comparable to that of larger trees, which are measured in the larger subplots. Without this adjustment, some disturbed forests with low tree densities might contain too few recorded individuals to robustly estimate size–abundance distributions.

Disturbance categories for plots were based on the classifications from the FIA condition-level data. FIA field crews delineate conditions on plots based on evidence of disturbance and a variety of other factors (e.g., forest edges, forest types and evidence of silvicultural treatments, among others). Based on these conditions, a plot is considered to be in a disturbed state if the area affected by the disturbance is $\geq$ 1 acre (0.4 ha) in size, with mortality or damage to $\geq$ 25% of the trees. Recorded disturbances must have occurred since the previous measurement (5–10 years depending on remeasurement period) or within 5 years of the initial plot installation (Burrill et al. 2021). We used disturbance codes from the FIA database to classify plots into the following categories: no disturbance, insect damage, human-caused damage (any significant threshold of human-caused damage not included in other disturbance or silvicultural categories. Logging is classified as an alternate silvicultural category), disease damage, fire (including both crown and ground fire), ground fire only, animal damage or grazing, and wind. FIA does not consider management and harvest events such as tree cutting, slash and burn, or clearing to be disturbances per se and instead classifies them as treatments. Such treatments are considered different from the 'human-caused damage' disturbance category. These classifications follow the FIA definitions and represent various natural and anthropogenic disturbances recorded in the database. We therefore removed plots that underwent treatments from our data to minimise the effect of confounding variables (10,774 plots).

Stand age and maximum tree height for a plot can significantly impact size-abundance slopes (Duncanson et al. 2015). In the FIA database, age estimates for each condition class in a plot are determined by calculating the average age of a subset of trees that have not been overtopped, selected from the size class that comprises the majority of trees in the forest canopy (Stevens et al. 2016; US Forest Service 2022). It is possible for a single plot to contain multiple conditions of different stand ages, so we computed the weighted mean of measured stand ages across the plot based on the condition proportion of each stand age within the plot. Maximum height was calculated by selecting the height of the largest live tree in the plot as measured by field crews with some form of instrument (e.g., clinometer, relascope, tape).

To determine the effect of disturbance on size-abundance slopes, we first needed to estimate the slope relating abundance to size (i.e., DBH) and its uncertainty for each plot. The slopes were estimated for each plot, irrespective of the species present.

Size-abundance distributions were modelled using a power law, which is commonly used to describe tree size distributions (Grady et al. 2024). This approach differs from traditional log–log regression in that it explicitly estimates the shape parameter (α) of the distribution rather than assuming a linear relationship in log-transformed data. We can then calculate log–log size-abundance slopes as equal to $-(\alpha+1)$ (Grady et al. 2024). We fit power-law distributions to the TPA-corrected data, using $x_{min}=3$ cm and removing measurements of trees with DBH <3 cm and >50 cm (Grady et al. 2024).

2.3 | Disturbance Effect: Bayesian Model

We then fit a Bayesian linear mixed-effects model to the corrected data from both the microplot and the subplot with the *brms* package in R (Bürkner 2017) using rstan as the back-end (Stan Development Team 2023) to examine the effect of disturbance type on slope, including stand age and maximum height as predictors. The model was estimated using Hamiltonian Markov Chain Monte Carlo (MCMC) sampling, with 9000 iterations, including a 6000-iteration warmup, and four chains. Prior distributions were defined for the model parameters, including normal distributions with a mean of zero and a standard deviation of five for population-level effects (b), and a mean of zero and a standard deviation of two for the parameter σ (i.e., residual error term). These are weakly informative priors that help to stabilise the sampling algorithm but do not add any information regarding the expected directionality of the relationship. We also included a random effect in the model to account for spatial variability using a conditional autoregressive (CAR) correlation structure. This random effect utilises 67 terrestrial ecoregions of The Nature Conservancy (2024), which allows the model to capture similarities between neighbouring ecoregions and adjust for spatial autocorrelation (Read et al. 2020). Draws were sampled using a No-U-Turn Sampler (NUTS, R v4.3.0, STAN v2.26.1). In our model, slope estimates are also associated with a degree of uncertainty, which we explicitly incorporate as measurement error into the model fitting process using the *mi()* function (following Kurz (2023)). This allows the model to more accurately reflect the variability and potential imprecision in the observed data, ensuring that our conclusions are robust to these uncertainties. The Bayesian model followed a Gaussian likelihood distribution with an identity link function. Most parameters demonstrated strong convergence diagnostics (R-hat ≈1.00, large ESS values), with the exception of the intercept, which exhibited a slightly elevated R-hat (1.04) and lower effective sample sizes (bulk-ESS = 203, tail-ESS = 128). Visual inspection of trace plots confirmed proper chain mixing for other parameters, while the intercept's behaviour suggests some additional uncertainty (Table S2, Figure S1). Prior sensitivity analysis, conducted using *priorsense* (Kallioinen et al. 2024), indicated that the posterior distribution was not sensitive to the chosen priors, further supporting that the results were primarily driven by the data (Table S3, Figure S2). The brms formula used to make this table is included in Table S2.

We first assessed the presence of an effect by calculating the probability that a parameter is strictly positive or negative, termed probability of direction (p_d) (Makowski et al. 2019). Unlike frequentist *p*-values, p_d is derived from Bayesian posterior estimates and provides a direct measure representing the certainty with which an effect goes in a particular direction; however, it is strongly correlated with the frequentist *p*-value. This metric focuses on the probability of observing a nonzero effect in the posterior distribution but does not account for whether that effect is practically meaningful. To assess practical significance, we then assessed the effects of disturbances on the response variable by calculating the proportion of the posterior distribution that falls within the Region of Practical Equivalence (p_{rope}) for each fixed-effect parameter, using the 'No Disturbance' category as the baseline for comparison. The p_{rope} defines an interval around a null effect, typically set at ±0.1 times the standard deviation of the response variable (SDy), following Kruschke (2018). This threshold corresponds to a 'small effect' as described in the Bayesian framework and is roughly analogous to Cohen's $d=0.1$. A high proportion of the posterior (close to 100%) within the p_{rope} suggests that the estimated effect is practically negligible, akin to failing to reject the null hypothesis in traditional hypothesis testing. Conversely, if little to none of the posterior falls within the p_{rope}, it indicates strong evidence for a meaningful effect of disturbance. By comparing each disturbance category against the 'No Disturbance' baseline, we can determine whether the estimated effects are credibly different from the undisturbed condition.

To explore this expectation further, we conducted a post hoc Bayesian mixed-effects analysis, focusing on plots affected by animal grazing or ground fires (the two disturbances with a significant effect on slope; see Results). Rather than limiting our data to the most recent surveys, we incorporated all available observations from 2001 to 2023 to better capture long-term trends. Our model estimates size-abundance slopes as a function of time since disturbance, stand age, disturbance type, and maximum height, while accounting for plot-level variability. This approach allows us to directly assess how size-abundance slopes evolve following disturbance events while controlling for stand characteristics and site-level variation. The Bayesian model followed a Gaussian likelihood distribution with an identity link function, and convergence diagnostics (Rhat = 1.00 for all parameters) confirmed the adequacy of the model fit. All parameters demonstrated strong convergence diagnostics (R-hat ≈1.00, large ESS values), and visual inspection of trace plots confirmed proper chain mixing (Table S4, Figure S3). Prior sensitivity analysis indicated that the posterior distribution was not sensitive to the chosen priors (Table S5, Figure S4). The brms formula used to make this table is included in Table S4.

2.4 | Disturbance Effect: Structural Equation Model

Finally, we fit a structural equation model (SEM) with the lavaan R package (Rosseel 2012) to decompose the effects of disturbance on the size–abundance slopes of forest stands, focusing specifically on the disturbance types identified as significant in our Bayesian model. SEMs extend multiple regression by allowing us to evaluate both direct and indirect effects among variables, which helps in understanding the

pathways through which disturbances affect forest structure. In our model, disturbance was included as a binary categorical variable with presence or absence, but only disturbance types that showed significant effects in the Bayesian analysis were retained. Because these disturbances primarily affected smaller trees, we assumed their overall effects on stand structure followed similar pathways. Specifically, we estimated direct effects of disturbance on stand age, maximum height, and slope, along with direct effects of stand age on both maximum height and slope. Indirect effects were modelled to capture how disturbances influence slope through their effect on stand age and maximum height.

The full model structure can be expressed by the following set of equations where letters represent parameters estimated:

$$\text{Max height} \sim a \times \text{disturbance} + b \times \text{stand age}$$

$$\text{Stand age} \sim c \times \text{disturbance}$$

$$\text{Slope} \sim d \times \text{disturbance} + e \times \text{max height} + f \times \text{stand age}$$

$$\text{Disturbance via stand age (Indirect)} := c \times f$$

$$\text{Disturbance via max height (Indirect)} := a \times e$$

$$\text{Stand age via max height (Indirect)} := b \times e$$

The total effects were calculated to account for both direct and indirect pathways. The total effect of disturbance on slope was computed as:

$$\text{Total impact of disturbance on slope} := d + (a \times e) + (c \times f) + (c \times b \times e)$$

Similarly, the total effect of stand age on slope was captured by:

$$\text{Total impact of stand age on slope} := f + (b \times e)$$

This model allowed us to disentangle the direct and indirect effects of disturbance and stand age on size-abundance slope, providing a more comprehensive view of how these factors shape forest structure.

3 | Results

The raw data used in our analysis included 4,539,963 individual trees of 409 species spread across 184,947 individual plots (Figure 2). Species richness varied across plots, with values ranging from 1 to 21 species per plot. The median species richness was 5, with an interquartile range of 3–7 species. The mean species richness was 5.35 (SD = 3.13). Plots represented 31 different forest types (note that 6% of the 163,588 plots used in the analysis did not have forest type classifications provided by FIA; Table S1). The most common forest types were oak/hickory (41,698 plots), pinyon/juniper (13,708 plots), and maple/beech/birch (12,705 plots). Stand age across the plots ranged from 1 to 860 years, with a median of 70 years, a mean of 78.73 years (SD = 53.68), and an interquartile range of 47–93 years. These data reflect a broad range of forest types and successional stages, from early succession to mature stands.

The majority of these plots experienced no disturbance (161,309), whereas the remaining plots were subject to various types of disturbances, including animal damage/grazing (4987 plots), disease damage (5288 plots), crown and ground fire (969 plots), ground-only fire (4166 plots), human-caused damage (1038 plots), insect damage (5215 plots), and wind (1975 plots) (Table 1). After applying the FIA TPA expansion factor to trees in both microplots and subplots, the analysis reflected a total of 113,710,359 trees and saplings (Figure 3).

In our Bayesian model of disturbance type (Bayesian $R^2 = 0.20$, Figure 4, Table 2), forests impacted by disturbances like animal damage, grazing, and ground fires, which predominantly remove smaller trees, exhibited shallower size-abundance slopes compared to undisturbed forests (Animal Damage/Grazing: $\beta = 0.13$, 95% CI: 0.12 to 0.14, $p_d = 100\%$; Ground Fire: $\beta = 0.15$, 95% CI: 0.13 to 0.16, $p_d = 100\%$; $p_{rope} = 0\%$). These disturbances create conditions where smaller trees are disproportionately negatively impacted, leading to a shift in forest structure. In contrast, disturbances such as disease damage, crown and ground fires, human-caused damage,

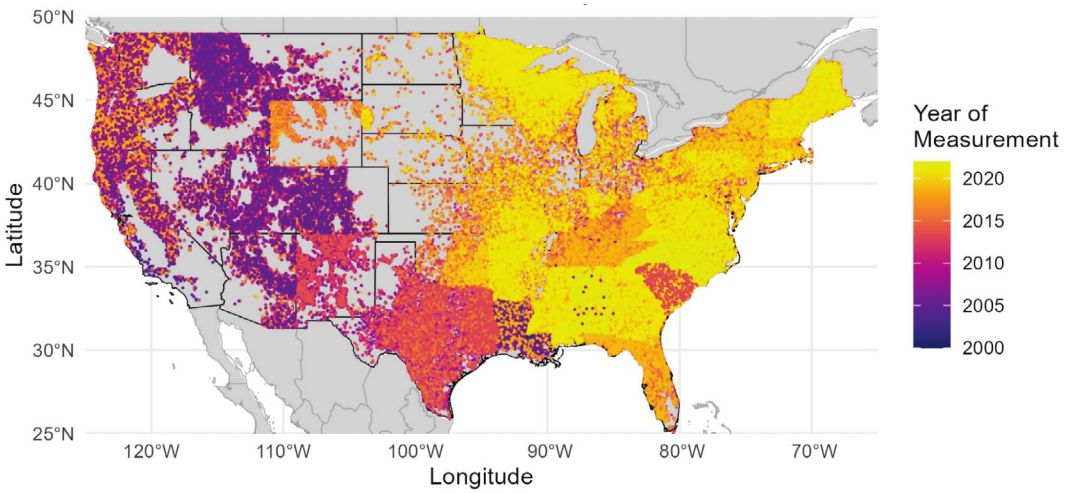

FIGURE 2 | Map of FIA survey points used in the analysis of this paper. The most recent survey for each plot was selected for analysis with the rFIA package. FIA sampling and data processing varies regionally, resulting in state-by-state differences in the most recent measurement year. This analysis included all available FIA plots, including intensified sampling plots in the western US from the early 2000s that are no longer sampled.

insect damage and wind showed no significant effects on the slope ($p_{rope} = 100\%$), suggesting these events may not substantially alter size distributions. The effects of disease damage and human-caused damage were present under the less conservative p_d estimate ($p_d = 99.99\%$). However, the effect size of disease damage was minimal, with a comparatively larger effect of human-caused damage (Table 2). Moreover, forests with older stand ages and taller maximum heights exhibited steeper slopes closer to −2, indicating that as forests age, they tend to develop structures closer to theoretical expectations (Stand Age: $\beta = 0.51$, 95% CI: 0.50 to 0.52, $p_d = 100\%$; Maximum Height: $\beta = 0.58$, 95% CI: 0.57 to 0.60, $p_d = 100\%$). Strong spatial autocorrelation was evident across the plots (CAR estimate = 0.92, 95% CI: 0.75 to 1.00).

TABLE 1 | The number of plots per disturbance type that fit our criteria in the FIA database.

Disturbance type	Number of plots
No disturbance	161,309
Animal damage/Grazing	4987
Disease damage	5288
Fire (Crown and ground)	969
Ground fire	4166
Human-caused damage	1038
Insect damage	5215
Wind	1975

Note: Plots that were not disturbed were the most prevalent in the dataset.

For the model examining the effect of disturbance over time (Figure 5), the linear term for time since disturbance revealed a weak negative relationship with size-abundance slopes (estimate = −0.01). This suggested that as time since disturbance increased, size-abundance slopes became progressively steeper—consistent with an initial lack of small trees followed by regeneration. Given that time since disturbance ranges from 0 to 20 years and size-abundance slopes are generally between 0 and 5, a small estimate is not unexpected. A 10-year increase in time since disturbance would correspond to a 0.1-unit change in slope, which is more meaningful in this context. However, this effect remains subtle, as indicated by the narrow credible interval (95% CI: −0.01 to −0.004), and the estimate fell entirely within the Region of Practical Equivalence ($p_{rope} = 100\%$), suggesting the effect is not practically significant despite the Probability of Direction ($p_d = 100\%$).

Stand age (log10-transformed) was included in the model as a control variable, but conditional effects plots (Figure 5) suggest that the influence of time since disturbance also depends on stand age. Size-abundance slopes are steeper overall in

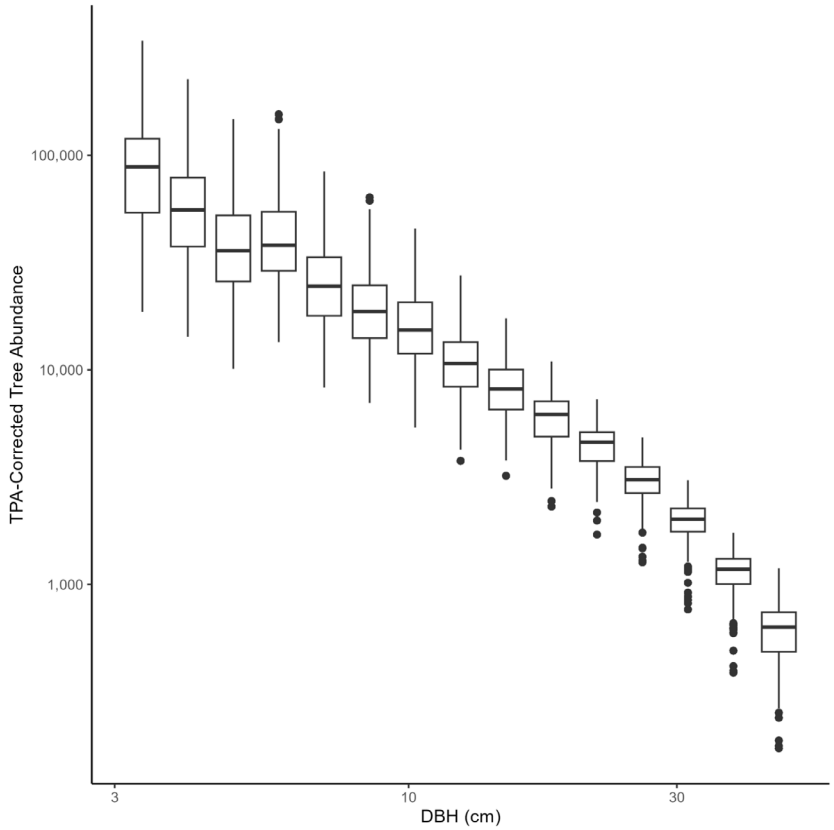

FIGURE 3 | Visual representation of tree size and abundance (number of stems) TPA-corrected FIA data, where abundance is calculated according to a logarithmic binning procedure (White et al. 2008). The figure includes all trees across the entire dataset, pooled from all plots that fall into the 'No Disturbance' category. The data are binned into 15 intervals based on the log-transformed tree diameter (DBH), with abundance calculated from the number of trees in each bin, corrected using the FIA TPA method. Raw tree data are counted multiple times by the FIA TPA correction to place abundance data from the microplots and the subplots on the same scale.

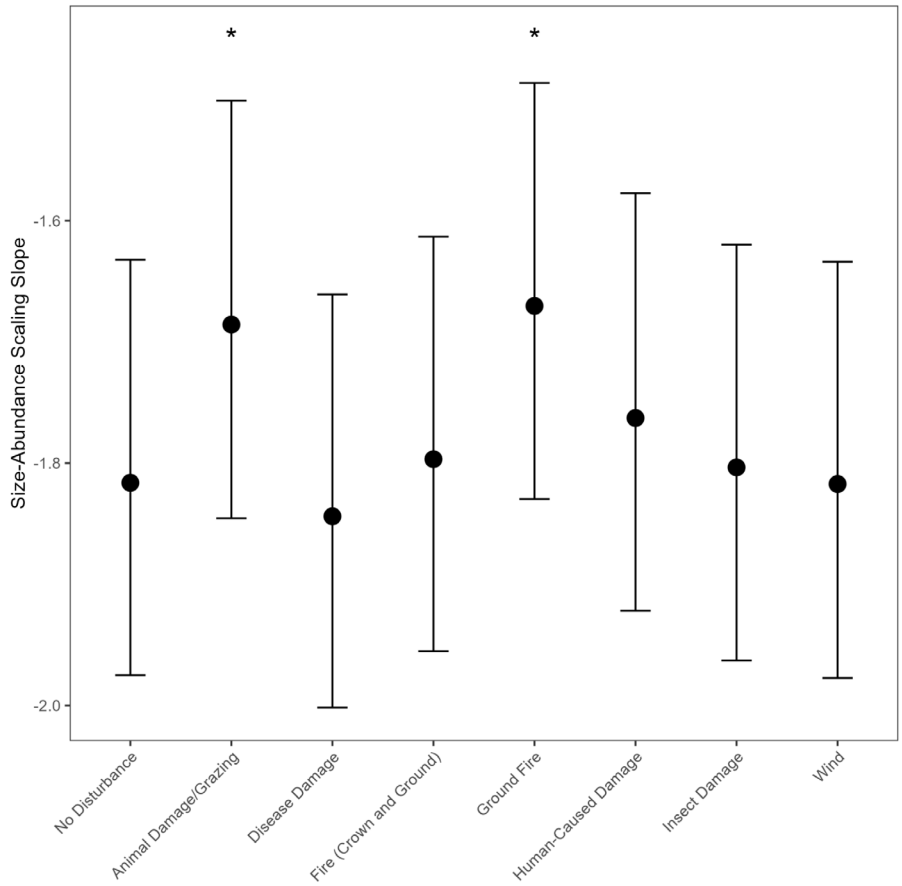

FIGURE 4 | Visualised conditional effects output from Bayesian model fit to both microplot and subplot data. Error bars are the posterior median and 95% credible interval, and the *y*-axis is split to magnify the error bars (Xu et al. 2021). Despite the wide range in possible size-abundance slopes, we found that animal grazing/damage and ground fires resulted in shallower slopes. Disturbance types classified as different from plots with no disturbance based on the p_{rope} are highlighted with an *.

younger stands compared to older stands, with both increasing in steepness at similar rates as time since disturbance increases (Figure 5). This suggests that younger stands may have initially had a steeper size-abundance slope—possibly reflecting a size structure dominated by smaller trees—while older stands exhibit a flatter slope at any given point in time since disturbance. The parallel increase in slope across stand ages suggests that post-disturbance recruitment and growth patterns are comparable, but younger stands maintain a consistently steeper size distribution.

Importantly, the inclusion of spatial autocorrelation in the updated model (CAR structure) accounted for spatial dependencies in the data. The CAR parameter estimate was 0.62 (95% CI: 0.06 to 0.97), indicating moderate spatial autocorrelation across plot-level intercepts. This suggests that the variation in size-abundance slopes is not entirely independent across plots and that neighbouring plots tend to share similar characteristics. The standard deviation for the CAR structure (sdcar) was estimated at 0.17 (95% CI: 0.13 to 0.23), further confirming the presence of spatial variability in the model's residuals. Plot-level variability remained modest, with the standard deviation of plot-level intercepts estimated at 0.23 (95% CI: 0.22 to 0.24). This corresponds to an Intraclass Correlation Coefficient (ICC) of approximately 0.26, indicating that 26% of the total variance in size-abundance slopes can be attributed to differences between plots, with the remaining 74% reflecting within-plot variation.

The results from the SEM (Figure 6, Table 3) support and build upon the findings of the size-abundance multiple regression model. The SEM is fully saturated (i.e., has zero degrees of freedom), meaning it exactly reproduces the observed covariance structure. As a result, traditional SEM fit indices (e.g., CFI, TLI, RMSEA, SRMR) are not informative. Instead, we assess the model based on parameter estimates and their associated uncertainty (Table 3). The direct effect of disturbance on the size-abundance slope (specifically the disturbance types with large effects from the Bayesian models, that is, Animal Damage/Grazing and Ground Fire) was significant, with a standardised coefficient (β) of 0.07 (95% CI: 0.06 to 0.08, $p < 0.001$) indicating that increased disturbance is associated with a shallower (i.e., less negative) slope. The direct effect of maximum height also demonstrated a significant positive effect on the slope ($\beta = 0.11$, 95% CI: 0.07 to 0.15, $p < 0.001$), as did the direct effect of stand age, which had a strong positive effect ($\beta = 0.36$, 95% CI: 0.31 to 0.41, $p < 0.001$). The indirect effects revealed that the path from disturbance through maximum height on slope was negligible ($\beta = 0.00$, 95% CI: 0.00 to 0.00, $p = 0.45$), as was the path from disturbance through stand age ($\beta = -0.01$, 95% CI: −0.01 to 0.00, $p = 0.22$). There was no direct effect of disturbance on maximum

TABLE 2 | Output of the Bayesian model fit to corrected subplot and microplot data.

Predictors	Estimates	CI (95%)	p_{rope}	p_d
Intercept	−3.87	−4.03 to −3.69	0.00%	100%
Stand age (log10)	0.51	0.50 to 0.52	0.00%	100%
Max height (log10)	0.58	0.57 to 0.60	0.00%	100%
Animal damage/ Grazing	0.13	0.12 to 0.14	0.00%	100%
Disease damage	−0.03	−0.04 to −0.01	100.00%	99.99%
Fire (Crown and ground)	0.02	-0.01 to 0.05	100.00%	90.33%
Ground fire	0.15	0.13 to 0.16	0.00%	100%
Human-caused damage	0.05	0.02 to 0.08	100.00%	99.99%
Insect damage	0.01	−0.00 to 0.03	100.00%	97.00%
Wind	0.00	−0.02 to 0.02	100.00%	53.72%
Observations			184,947	

Note: The percent of the posterior within the p_{ROPE} provides a more conservative estimate of effect prevalence compared to the probability of direction p_d.

height ($\beta = 0.01$, 95% CI: −0.02 to 0.04, $p = 0.47$), whereas there was a direct effect of stand age on maximum height ($\beta = 0.18$, 95% CI: 0.01 to 0.35, $p = 0.04$). The total effect of stand age on the slope was substantial ($\beta = 0.38$, 95% CI: 0.35 to 0.41, $p < 0.001$), indicating a strong influence of stand age on the size-abundance relationship. Overall, these findings highlight the significant roles of both stand age and maximum height in shaping size-abundance slopes, while also demonstrating a measurable effect of disturbance.

4 | Discussion

Disturbance regimes play a fundamental role in shaping forest structure, with lasting impacts on tree size distributions that influence long-term trajectories of forest dynamics (Seidl et al. 2014; Seidl and Turner 2022; Grady et al. 2024). Our study demonstrates that different disturbance types drive distinct changes in size-abundance relationships, with size classes responding predictably based on disturbance severity and selectivity. Disturbances that are known to disproportionately affect smaller trees, such as ground fires and animal grazing, were associated with shallower size-abundance slopes. This is consistent with our hypothesis that disturbances will cause predictable deviations from the theoretical equilibrium slope, even for older forests. As the forest recovers, recruitment and growth of new small trees should drive the slope back towards the theoretical equilibrium (Enquist et al. 2009; Zhou et al. 2021). However, increasing disturbance regimes are pushing many forests towards shorter-statured and younger stands, suggesting that a true equilibrium may be less commonly achieved in many of the world's recovering forests (McDowell et al. 2020). This aligns with a growing understanding that disturbed forests may not simply ecoverto historical conditions but rather undergo a process of eorganisation (Seidl and Turner 2022) leading to novel ecosystem states that diverge from pre-disturbance conditions (Swanson et al. 2011).

In contrast to disturbances that selectively remove smaller trees, we found that disturbances impacting trees more uniformly across size classes exhibited limited effects on slope. This suggests that the size selectivity of disturbance is a key determinant of forest recovery trajectories. Disturbances that may not remove trees from the landscape (e.g., insect or disease damage) have a lag effect not immediately visible (e.g., insect or disease damage) or impact trees of all sizes (e.g., crown and ground fires together) had no or limited effect on slope in comparison to plots with no disturbance. The only disturbance type that appeared to violate this trend was wind. As shown in Figure 1, we expected wind to have a significant effect on slope compared to undisturbed plots. However, our analysis found no difference between wind-disturbed plots and those without disturbance. This may reflect limitations in the FIA disturbance classification, which groups diverse wind events—ranging from localised windthrow to large-scale storms—under a single category (Fitts et al. 2022). These differing effects may offset one another, masking any clear relationship between wind disturbance and size-abundance slope.

This pattern of predictable shifts in size-abundance slopes following disturbance connects to a broader body of work examining the scaling relationships of tree size distributions. The search for general scaling patterns in ecology has a long history, with several proposed interacting mechanisms such as volume packing constraints (De Liocourt 1898; Yoda et al. 1963), stochastic packing theory (Taubert et al. 2015), growth-mortality trade-offs (Muller-Landau et al. 2006), energy availability (Damuth 1981; West et al. 2009), and light limitation in canopy gaps (Farrior et al. 2016). The mechanisms behind scaling theory are still debated (Enquist et al. 2009; Farrior et al. 2016; Muller-Landau et al. 2006; West et al. 2009). Disturbance history in particular is cited as a large reason for why forests may not adhere to size-abundance equilibria predictions (Coomes et al. 2003; Coomes and Allen 2007), to the point where modern-day disequilibrium in forests may reflect legacies of past disturbance events (Coomes and Allen 2007). We demonstrate that these perturbations still have a predictable directionality on how they impact size-abundance distribution slopes, with disturbances that selectively remove smaller trees leading to shallower slopes, whereas those that impact all size classes more uniformly have less of an effect on theslope.

Regardless of the disturbance type, stand age and maximum tree height were consistent predictors of size-abundance slopes, aligning with Duncanson et al. (2015). Our models indicate that younger forests with smaller trees tend to exhibit steeper slopes, whereas older forests with larger trees show shallower

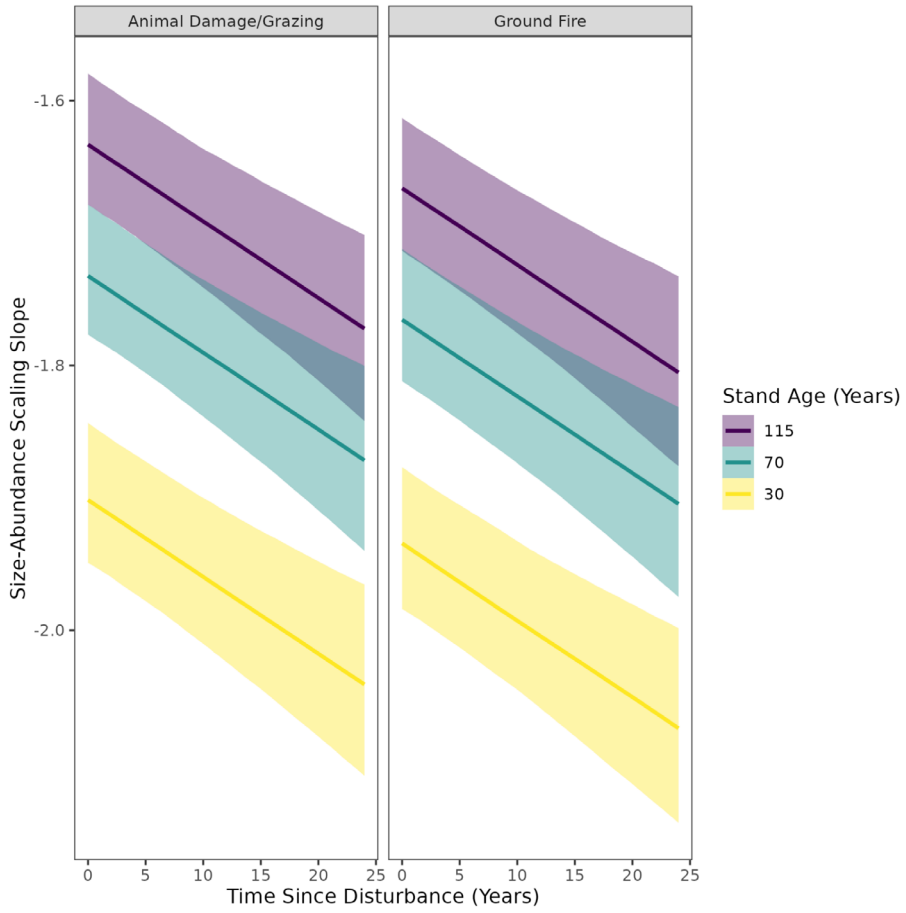

FIGURE 5 | Size-abundance scaling slopes fit with a Bayesian smoothing term (*brms* uses generalised additive models) to show the influence of time since disturbance in years on slopes. Plots are included as a random effect. The shading indicates the 95% CI.

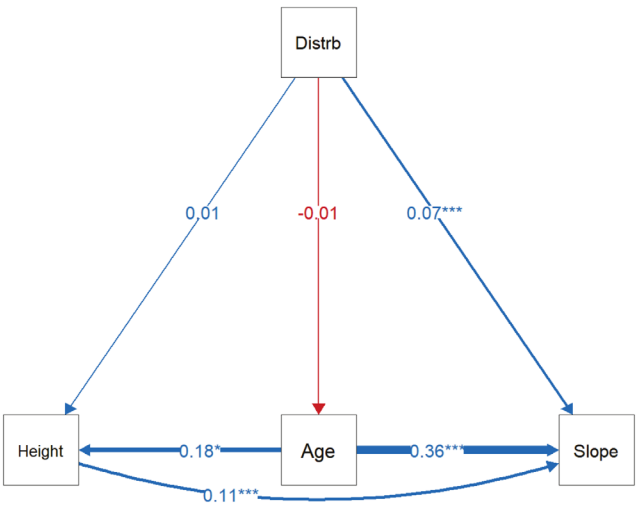

FIGURE 6 | Diagram of the structural equation model. Indirect effects and net effects (indirect + direct) are not included in the diagram, but are provided in Table 3. Significance values are displayed as $^{*}p < 0.05$; $^{***}p < 0.001$. Exact *p*-values for each relationship are also provided in Table 3. Disturbance is abbreviated as 'Distrb.' Red indicates negative relationships, whereas blue indicates positive relationships. Arrow thickness indicates the strength of the relationship, represented numerically by the numbered label.

slopes. Furthermore, the SEM reveals that the relative effects of stand age and maximum tree height are more critical for predicting size-abundance slopes than disturbance types. Although we might expect this to be because of disturbance impacting slope indirectly through stand age and maximum height, there were no direct effects of disturbance on stand age or maximum height. However, although the strength of disturbance on size-abundance slopes is relatively lower than stand age and maximum tree height, it nonetheless results in shallower slopes for animal grazing and ground fires. This suggests that while forest development plays a dominant role in shaping size structure, disturbance can still exert a significant influence, particularly when it selectively targets smaller trees.

Our focus on size-abundance distributions, rather than looking at changes in average tree size over time, allows us to capture the full complexity of how disturbance reshapes forest structure. While average tree size can provide a general indication of growth or mortality trends, it obscures the critical shifts in the relative proportions of different size classes within the population. For instance, a change in average tree size could result from the loss of small trees, the growth of large trees, or a combination of both—outcomes that have very different implications for forest dynamics and carbon storage. In contrast, shifts in the size-abundance slope directly reflect the underlying processes

TABLE 3 | Standardised regression coefficients for the direct and indirect effects of disturbance, stand age and maximum height on size-abundance slope from the structural equation model.

		Standardised					
Predictor	**Effect**	***β***	**95% CI**	**SE**	***z***	***p***	**sig**
Disturbance	Indirect on slope via maximum height	0.00	0.00 to 0.00	0	0.75	0.45	
Disturbance	Indirect on slope via stand age	−0.01	−0.01 to 0.00	0.01	−1.24	0.22	
Disturbance	Direct on maximum height	0.01	−0.02 to 0.04	0.03	0.72	0.47	
Stand age	Direct on maximum height	0.18	0.01 to 0.35	0.07	2.11	0.04	*
Disturbance	Direct on stand age	−0.01	−0.04 to 0.01	0.01	−1.27	0.20	
Stand age	Indirect on slope via maximum height	0.02	0.00 to 0.04	0.01	1.68	0.09	
Disturbance	Direct on slope	0.07	0.06 to 0.08	0.01	10.49	< 0.001	***
Maximum height	Direct on slope	0.11	0.07 to 0.15	0.03	4.84	< 0.001	***
Stand age	Direct on slope	0.36	0.31 to 0.41	0.02	14.87	< 0.001	***
Disturbance (Net Effect)	Direct on slope	0.06	0.05 to 0.08	0.01	7.87	< 0.001	***
Stand age (Net Effect)	Direct on slope	0.38	0.35 to 0.41	0.02	23.75	0.00	***

Note: Indirect effects are mediated through either stand age or maximum height, with 95% confidence intervals (CI), standard errors (SE), *z*-values, and *p*-values reported. Significant effects are indicated with asterisks: *$p < 0.05$, **$p < 0.01$, ***$p < 0.001$. Net effects represent the total impact of disturbance and stand age on the slope, combining direct and indirect pathways.

of recruitment, mortality, and changes in demographic structure driven by disturbance or competition (Grady et al. 2024). As illustrated by our analysis of ground fire effects (Figure 5), examining the scaling slope reveals a surge in recruitment and/or enhanced growth of smaller individuals, a pattern that would be difficult to discern from changes in average tree size alone. This detailed understanding of how disturbance reshapes forest structure is crucial because many key forest ecosystem properties, including resilience and carbon cycling, emerge from the complex and reciprocal interactions between forest structure and disturbance (Mitchell et al. 2023).

The lack of effect of disturbance on maximum height is likely because the disturbances examined in the SEM predominantly affect smaller trees, resulting in shallower slopes without impacting the largest trees. The lack of effect of disturbance on stand age, on the other hand, may stem from the way stand age is measured by the FIA programme rather than reflecting a true ecological pattern (Stevens et al. 2016). The FIA programme estimates stand age based on the average age of a subset of non-overtopped trees selected from the DBH size class that represents the plurality of dominant and co-dominant trees in the forest overstory (US Forest Service 2022). Consequently, FIA stand age does not necessarily account for the oldest trees (Stevens et al. 2016). If stand age included these individuals, we would expect disturbances that impact smaller trees (and lead to shallower size-abundance slopes) to increase the average stand age due to the loss of younger trees while older trees remain. However, since the FIA methodology excludes the abundance of older trees and the complex age structure within plots and surrounding stands, any potential disturbance effects on stand age are likely obscured (Stevens et al. 2016).

Similarly, constraints in capturing variation in time since disturbance likely influence observed changes in size-abundance slopes over time. Our results suggest that size-abundance slopes steepen in the decades following a disturbance, reflecting the recruitment and growth of smaller trees into the gaps created by the disturbance. To clarify, a severe disturbance can initially flatten the slope, even to near zero, if many trees are removed. As succession proceeds and new trees establish, the slope then progressively steepens towards an equilibrium state. This post-disturbance recovery, characterised by the establishment and growth of new individuals, is often facilitated by disturbance legacies (e.g., surviving trees) which play a critical role in increasing the resilience of forest ecosystem structure and function (Seidl et al. 2014). The steepening, however, is a subtle effect in the analysis, with the estimated relationship between time since disturbance and slope being weakly negative and the credible interval including zero, indicating substantial uncertainty. This variability likely arises from the limited number of plots with longer time since disturbance; only 2.04% of disturbed plots in our analysis were recorded as being more than 15 years post-disturbance. This is likely a limitation of the FIA data, as remeasurements tend to cover a maximum of 10–20 years. Notably, all western U.S. plots have only one 10-year remeasurement, with an additional 5 years of prior disturbance included in the first measurement, resulting in a total of 15 years at maximum. In contrast, some eastern U.S. plots may have four or more remeasurements (e.g., 2000, 2007, 2014, 2021), plus 5 years of prior disturbance, yielding a total of 26 years at maximum. Our results also suggest that the effect of time since disturbance is not uniform across all conditions but may depend on stand age at the time of disturbance. Conditional effects plots indicate that younger stands exhibit steeper size-abundance slopes overall compared to older stands, and this pattern is maintained across time since disturbance. Both younger and older stands appear to steepen in slope at similar rates following disturbance, suggesting that post-disturbance recruitment and growth patterns are comparable across age classes, but younger stands consistently reflect a size structure dominated by smaller trees. Future analyses could benefit from examining the effect of time since

disturbance separately by disturbance type, as different disturbance agents (e.g., fire, wind, harvesting) likely produce different initial conditions and rates of recovery. Additionally, as the FIA program continues to remeasure plots over longer time periods, we anticipate that the uncertainty surrounding this effect will decrease, allowing for more robust detection of temporal changes in size-abundance relationships.

In addition to constraints surrounding time since disturbance in the observed data, there is also a bias towards moderate disturbances. FIA measures disturbances at the condition level, which requires over 25% of trees to be damaged or dead within an area larger than one acre. While this threshold is practical for field crews to identify large-scale disturbances, such as fires or tornadoes, it likely misses more minor disturbances (Fitts et al. 2022). Similarly, our methods required a minimum number of trees to be present after disturbance to estimate a size-abundance slope, so some large-scale, stand-clearing disturbances were not included in our analysis. Our focus on moderate disturbances may limit our ability to detect the subtler impacts of smaller-scale events on forest structure. Future studies should explore the effects of these smaller disturbances, perhaps by integrating more sensitive detection methods.

It is important to recognise that the dynamics of large tree loss may be underestimated in this study. The large sample size of the FIA programme, which spans multiple forest types and ownerships, offers a robust representation of general forest trends, but our focus on sub- and microplot trees, excluding larger trees, may miss significant aspects of the large tree loss narrative often discussed in the literature. However, this does not undermine the broader relevance of our findings, as they align with established patterns in forest size structure (Enquist et al. 2009; Farrior et al. 2016; Zhou et al. 2021; Grady et al. 2024). Furthermore, research on forest structure and disturbance has increasingly emphasised the importance of considering the interactions between disturbance type, severity and the pre-disturbance forest structure in shaping post-disturbance trajectories (Seidl et al. 2014; Haber et al. 2020). Our findings contribute to this understanding by demonstrating how the size selectivity of disturbance, in conjunction with stand age and maximum height, influences the directionality of shifts in size-abundance relationships.

5 | Conclusions

Our findings suggest that a flattening in the size-abundance relationship is common following targeted disturbances such as ground fire and animal damage, indicating that widespread disturbances may disproportionately impact smaller trees across the contiguous U.S. Slopes in areas with targeted disturbances potentially steepen over time due to regrowth. While a shallower slope could theoretically result if the largest trees continue growing while the abundance of small trees remains the same, such a pattern is ecologically unlikely. In contrast, disturbances that do not selectively target tree sizes produce less predictable changes in slope patterns. These shifts in forest structure and demographics affect successional stages and carbon trajectories. As disturbance frequency and intensity rise due to changes in forest management, land use, and climate, understanding these dynamics becomes increasingly critical. Further research into how disturbances interact with environmental gradients will be essential for developing effective forest carbon management strategies.

Acknowledgements

We thank Brian Walters (NRS FIA) and Glenn Christensen (PNW FIA) for providing critical information regarding the inclusion of FIA trees within macroplots, which were excluded from our subplot measurements. We also thank the countless FIA crew members and information management staff who collected and compiled this data. This research was supported by NASA's Biodiversity and Ecological Conservation programme (grant 80NSSC23K0421), by Hatch project award no. [MEO-022425], from the U.S. Department of Agriculture's National Institute of Food and Agriculture, and the Northeastern States Research Cooperative through funding made available by the USDA Forest Service. This research was also supported by the U.S. Department of Agriculture Forest Service, Northern Research Station, Forest Inventory and Analysis Programme. The conclusions and opinions in this paper are those of the authors and not of the NSRC, the Forest Service or the USDA.

Conflicts of Interest

The authors declare no conflicts of interest.

Data Availability Statement

The data that support the findings of this study are available in the FIA database at https://research.fs.usda.gov/products/dataandtools/tools/fia-datamart. We recommend using the rFIA R package to download FIA data. The R and Stan code used to analyse these data is available at https://github.com/ForestScaling/DisturbanceSizeScaling (https://doi.org/10.5281/zenodo.15664089). Data are available at https://doi.org/10.5281/zenodo.15676017.

References

Bechtold, W. A., and P. L. Patterson. 2005. *The Enhanced Forest Inventory and Analysis Program—National Sampling Design and Estimation Procedures*. USDA Forest Service, Southern Research Station.

Belgrano, A., A. P. Allen, B. J. Enquist, and J. F. Gillooly. 2002. "Allometric Scaling of Maximum Population Density: A Common Rule for Marine Phytoplankton and Terrestrial Plants." *Ecology Letters* 5: 611–613.

Bürkner, P.-C. 2017. "Brms: An R Package for Bayesian Multilevel Models Using Stan." *Journal of Statistical Software* 80: 1–28.

Burrill, E. A., A. M. DiTommaso, J. A. Turner, et al. 2021. The Forest Inventory and Analysis Database: Database Description and User Guide for Phase 2 (version 9.0).

Coomes, D. A., and R. B. Allen. 2007. "Mortality and Tree-Size Distributions in Natural Mixed-Age Forests." *Journal of Ecology* 95, no. 1: 27–40.

Coomes, D. A., R. P. Duncan, R. B. Allen, and J. Truscott. 2003. "Disturbances Prevent Stem Size-Density Distributions in Natural Forests From Following Scaling Relationships: Scaling Rules and Size-Density Distributions." *Ecology Letters* 6: 980–989.

Damuth, J. 1981. "Population Density and Body Size in Mammals." *Nature* 290: 699–700.

De Liocourt, F. 1898. "De l'aménagement des sapinières." *Bulletin Trimestriel - Société Forestière de Franche-Comté & Belfort* 4: 396–409.

Domke, G. M., B. F. Walters, D. J. Nowak, et al. 2023. "Greenhouse Gas Emissions and Removals From Forest Land, Woodlands, and Urban Trees in the United States, 1990–2021." In *Resource Update FS–307*, 5. U.S. Department of Agriculture, Forest Service, Northern Research Station.

Duncanson, L. I., R. O. Dubayah, and B. J. Enquist. 2015. "Assessing the General Patterns of Forest Structure: Quantifying Tree and Forest Allometric Scaling Relationships in the United States." *Global Ecology and Biogeography* 24: 1465–1475.

Enquist, B. J., G. B. West, and J. H. Brown. 2009. "Extensions and Evaluations of a General Quantitative Theory of Forest Structure and Dynamics." *Proceedings of the National Academy of Sciences* 106: 7046–7051.

Farrior, C. E., S. A. Bohlman, S. Hubbell, and S. W. Pacala. 2016. "Dominance of the Suppressed: Power-Law Size Structure in Tropical Forests." *Science* 351: 155–157.

Fei, S., I. Jo, Q. Guo, et al. 2018. "Impacts of Climate on the Biodiversity-Productivity Relationship in Natural Forests." *Nature Communications* 9: 5436.

Fitts, L. A., G. M. Domke, and M. B. Russell. 2022. "Comparing Methods that Quantify Forest Disturbances in the United States' National Forest Inventory." *Environmental Monitoring and Assessment* 194: 1–17.

Grady, J. M., Q. D. Read, S. Record, et al. 2024. "Life History Scaling in a Tropical Forest." *Journal of Ecology* 112: 487–500.

Haber, L. T., R. T. Fahey, S. B. Wales, et al. 2020. "Forest Structure, Diversity, and Primary Production in Relation to Disturbance Severity." *Ecology and Evolution* 10: 4419–4430.

Kallioinen, N., T. Paananen, P.-C. Bürkner, and A. Vehtari. 2024. "Detecting and Diagnosing Prior and Likelihood Sensitivity With Power-Scaling." *Statistics and Computing* 34: 57.

Kellner, J. R., and G. P. Asner. 2009. "Convergent Structural Responses of Tropical Forests to Diverse Disturbance Regimes." *Ecology Letters* 12: 887–897.

Knott, J. A., M. A. Jenkins, C. M. Oswalt, and S. Fei. 2020. "Community-Level Responses to Climate Change in Forests of the Eastern United States." *Global Ecology and Biogeography* 29: 1299–1314.

Kruschke, J. K. 2018. "Rejecting or Accepting Parameter Values in Bayesian Estimation." *Advances in Methods and Practices in Psychological Science* 1, no. 2: 270–280.

Kurz, S. A. 2023. *Missing Data and Other Opportunities*. 2nd ed. Statistical Rethinking with brms, ggplot2, and the tidyverse.

Makowski, D., M. S. Ben-Shachar, S. A. Chen, and D. Lüdecke. 2019. "Indices of Effect Existence and Significance in the Bayesian Framework." *Frontiers in Psychology* 10: 2767.

McDowell, N. G., C. D. Allen, K. Anderson-Teixeira, et al. 2020. "Pervasive Shifts in Forest Dynamics in a Changing World." *Science* 368: eaaz9463.

Mitchell, J. C., D. M. Kashian, X. Chen, et al. 2023. "Forest Ecosystem Properties Emerge From Interactions of Structure and Disturbance." *Frontiers in Ecology and the Environment* 21: 14–23.

Muller-Landau, H. C., R. S. Condit, K. E. Harms, et al. 2006. "Comparing Tropical Forest Tree Size Distributions With the Predictions of Metabolic Ecology and Equilibrium Models." *Ecology Letters* 9: 589–602.

Oswalt, S. N., W. B. Smith, P. D. Miles, and S. A. Pugh. 2019. "Forest Resources of the United States, 2017: A Technical Document Supporting the Forest Service 2020 RPA Assessment." In *Gen. Tech. Rep. WO-97*, 97. Department of Agriculture, Forest Service, Washington Office.

Perkins, D. M., A. Perna, R. Adrian, et al. 2019. "Energetic Equivalence Underpins the Size Structure of Tree and Phytoplankton Communities." *Nature Communications* 10: 255.

Piponiot, C., K. J. Anderson-Teixeira, S. J. Davies, et al. 2022. "Distribution of Biomass Dynamics in Relation to Tree Size in Forests Across the World." *New Phytologist* 234: 1664–1677.

Read, Q. D., P. L. Zarnetske, S. Record, et al. 2020. "Beyond Counts and Averages: Relating Geodiversity to Dimensions of Biodiversity." *Global Ecology and Biogeography* 29: 696–710.

Rosseel, Y. 2012. "Lavaan: An R Package for Structural Equation Modeling." *Journal of Statistical Software* 48: 1–36.

Seidl, R., W. Rammer, and T. A. Spies. 2014. "Disturbance Legacies Increase the Resilience of Forest Ecosystem Structure, Composition, and Functioning." *Ecological Applications* 24: 2063–2077.

Seidl, R., D. Thom, M. Kautz, et al. 2017. "Forest disturbances under climate change." *Nature Climate Change* 7: 395–402.

Seidl, R., and M. G. Turner. 2022. "Post-Disturbance Reorganization of Forest Ecosystems in a Changing World." *Proceedings of the National Academy of Sciences of the United States of America* 119: e2202190119.

Smith, W. B. 2002. "Forest Inventory and Analysis: A National Inventory and Monitoring Program." *Environmental Pollution* 116: S233–S242.

Stan Development Team. 2023. RStan: the R interface to Stan.

Stanke, H., A. O. Finley, A. S. Weed, B. F. Walters, and G. M. Domke. 2020. "rFIA: An R Package for Estimation of Forest Attributes With the US Forest Inventory and Analysis Database." *Environmental Modelling & Software* 127: 104664.

Stevens, J. T., H. D. Safford, M. P. North, et al. 2016. "Average Stand Age From Forest Inventory Plots Does Not Describe Historical Fire Regimes in Ponderosa Pine and Mixed-Conifer Forests of Western North America." *PLoS One* 11: e0147688.

Swanson, M. E., J. F. Franklin, R. L. Beschta, et al. 2011. "The Forgotten Stage of Forest Succession: Early-Successional Ecosystems on Forest Sites." *Frontiers in Ecology and the Environment* 9: 117–125.

Taubert, F., M. W. Jahn, H.-J. Dobner, T. Wiegand, and A. Huth. 2015. "The Structure of Tropical Forests and Sphere Packings." *Proceedings of the National Academy of Sciences* 112: 15125–15129.

The Nature Conservancy. 2024. *The Nature Conservancy Terrestrial Ecosystems*. TNC Geospatial Conservation Atlas. https://geospatial.tnc.org/.

Tinkham, W. T., P. R. Mahoney, A. T. Hudak, et al. 2018. "Applications of the United States Forest Inventory and Analysis Dataset: A Review and Future Directions." *Canadian Journal of Forest Research* 48: 1251–1268.

US Forest Service. 2022. Forest Inventory and Analysis National Core Field Guide Volume I: Field Data Collection Procedures for Phase 2 Plot.

West, G. B., B. J. Enquist, and J. H. Brown. 2009. "A General Quantitative Theory of Forest Structure and Dynamics." *Proceedings of the National Academy of Sciences* 106: 7040–7045.

White, E. P., B. J. Enquist, and J. L. Green. 2008. "On Estimating the Exponent of Power-Law Frequency Distributions." *Ecology* 89: 905–912.

Xu, S., M. Chen, T. Feng, L. Zhan, L. Zhou, and G. Yu. 2021. "Use Ggbreak to Effectively Utilize Plotting Space to Deal With Large Datasets and Outliers." *Frontiers in Genetics* 12: 774846.

Yoda, K., T. Kira, H. Ogawa, and K. Hozumi. 1963. "Self-Thinning in Overcrowded Pure Stands Under Cultivated and Natural Conditions." *Journal of Biology* 14: 107–129.

Zhang, W.-P., E. C. Morris, X. Jia, S. Pan, and G.-X. Wang. 2015. "Testing Predictions of the Energetic Equivalence Rule in Forest Communities." *Basic and Applied Ecology* 16: 469–479.

Zhou, J., K. Yu, G. Lin, and Z. Wang. 2021. "Variance in Tree Growth Rates Provides a Key Link for Completing the Theory of Forest Size Structure Formation." *Journal of Theoretical Biology* 529: 110857.

Supporting Information

Additional supporting information can be found online in the Supporting Information section. **Data S1:** Supporting Information.